Radiation-induced defects in electron-irradiated γ-TiAl compounds: the effect of composition

1997 J. Phys.: Condens. Matter 9 5527

(http://iopscience.iop.org/0953-8984/9/26/003)

J. Phys.: Condens. Matter **9** (1997) 5527–5541. Printed in the UK PII: S0953-8984(97)77783-X

Radiation-induced defects in electron-irradiated γ-TiAl compounds: the effect of composition

G Sattonnay, F Ma†, C Dimitrov and O Dimitrov

CECM-CNRS, 15 rue Georges Urbain, F 94407 Vitry-sur-Seine Cédex, France

Received 12 September 1996, in final form 7 March 1997

Abstract. The radiation damage produced at 21 K by 2.5 MeV electrons, and the subsequent recovery have been investigated for γ-TiAl intermetallic compounds (50–54.5 at.% Al) by means of residual electrical resistivity measurements, with particular emphasis on the effects of the composition and fluence. The resistivity damage rate was much higher for the alloys than for a simultaneously irradiated nickel reference sample. Disordering contributes only a small fraction (8–15%) to the resistivity damage. The analysis of the dominant defect contribution led to Frenkel-pair resistivity values of $\approx$60 $\mu\Omega$ cm/%, larger than those for pure Al or Ti, and nearly independent of the composition. The recovery of the damage was characterized by two main stages. The temperature of the first one ($\approx$81 K) is independent of the composition: it was assigned to close-pair recombination, and to the migration and annihilation of self-interstitials. The second main one ($\approx$444 K, for the stoichiometric compound) has a temperature which depends on the fluence and on the composition. It corresponds to the migration and elimination of vacancies. An activation enthalpy of 1.55 ± 0.16 eV was estimated for this stage for stoichiometric TiAl. Its shift to higher temperatures with increasing aluminium content indicates a reduction in the vacancy mobility.

1. Introduction

TiAl-based intermetallic compounds are attractive candidates as regards high-temperature applications in the aerospace and automobile industries. Some important high-temperature characteristics of these materials, such as creep resistance and microstructural stability, are related to the atomic mobility via vacancy diffusion. Therefore, it is essential to obtain data on the diffusion characteristics and on the vacancy properties.

Diffusion in γ-TiAl has been considered in a number of publications. An activation enthalpy of $Q = 3.02$ eV for titanium self-diffusion was derived from measurements of the diffusion of ^{44}Ti in a $Ti_{46}Al_{54}$ alloy, with a pre-exponential factor $D_0 = 1.53 \times 10^{-4}$ m^2 s^{-1} (Kroll *et al* 1992). It was concluded that diffusion in γ-TiAl occurred via a vacancy mechanism like in fcc metals. Some interdiffusion experiments have been carried out on single-phase $Ti_{50}Al_{50}/Ti_{46}Al_{54}$ couples (Sprengel *et al* 1996). These showed that the temperature dependence of the interdiffusivity followed an Arrhenius law, with a pre-exponential factor $D_0 = 2.8 \times 10^{-4}$ m^2 s^{-1} and an activation enthalpy $Q = 3.06 \pm 0.10$ eV. Interdiffusion measurements performed on multi-phase couples (Hirano and Iijima 1984) have yielded higher diffusivities and lower activation enthalpies.

† Permanent address: Institute of Modern Physics, Academia Sinica, 253 Nanchang Road, 730000 Lanzhou, People's Republic of China.

0953-8984/97/265527+15$19.50

For the lattice vacancies, an effective vacancy formation enthalpy of 1.41 ± 0.06 eV for a γ-$Ti_{48.5}Al_{51.5}$ alloy was deduced from high-temperature positron lifetime measurements (Brossmann *et al* 1994) in the range 300–1400 K. This gives a thermal vacancy concentration of 1.5×10^{-4} for γ-TiAl at the melting temperature (1726 K), a value similar to the concentrations existing in pure metals.

Information on vacancy migration properties can be obtained from irradiation experiments. Also, irradiation effects are important, since TiAl compounds have recently been considered as potential nuclear materials (Mori *et al* 1992), due to their high creep resistance and to their low neutron-induced radioactivity as compared to that of stainless steels. However, the effects of irradiation on γ-TiAl have been little investigated, and very limited data are available. Some results were obtained by positron lifetime measurements on $Ti_{51}Al_{49}$, $Ti_{48}Al_{52}$, and $Ti_{44}Al_{56}$ samples irradiated below 160 K with 10 MeV electrons and at room temperature with 2 MeV protons (Shirai and Yamaguchi 1992). Two stages in the variation of the positron lifetime were observed for electron- and proton-irradiated samples: the first stage at 250 K was attributed to vacancy migration, and the second between 400 and 800 K was assigned to the elimination of dislocation loops or collapsed planar defects. Recently, vacancies in a $Ti_{48.5}Al_{51.5}$ alloy were also investigated by means of positron lifetime measurements after irradiation at 140 K with 0.55 MeV electrons and at 95 K with 2.5 MeV electrons (Würschum *et al* 1996). During isochronal anneals, the mean positron lifetime displayed an important decrease at 450 K, which was assigned to vacancy migration. In other experiments, after neutron irradiation of a $Ti_{44}Al_{56}$ sample at a temperature below 360 K, a first recovery stage below 660 K was attributed to the elimination of collapsed planar aggregates (dislocation loops), and the second stage above 660 K to the dissolution of submicroscopic voids (Shirai *et al* 1996). All irradiation damage annealed out below 800 K for electron- and proton-irradiated samples, and below 960 K for neutron-irradiated samples.

The aim of the present work was:

(i) to perform a thorough investigation of defect production and recovery for irradiated TiAl, particularly in the domain of low temperatures, which has not been studied until now;

(ii) to use electrical resistivity measurements in order to obtain a deeper insight into the processes occurring during electron irradiation and during subsequent annealing; and

(iii) to determine the effect of alloy composition on the damage production and recovery.

Single-phase γ-TiAl intermetallic compounds with 50, 51.5, 53, and 54.5 at.% Al were investigated. Low-temperature electron irradiations were used for introducing point defects, and the resulting damage was monitored by means of residual electrical resistivity measurements. The defect production and disordering processes taking place during irradiation will be discussed, and we will attempt to evaluate the Frenkel-pair resistivity in γ-TiAl. Next, the recovery during isochronal anneals will be determined, yielding information on the mobility of self-interstitials and vacancies.

2. Experimental procedure

Binary TiAl alloys containing 50, 51.5, 53, and 54.5 at.% Al were investigated. They will be respectively referred to as $TiAl_{50}$, $TiAl_{51.5}$, $TiAl_{53}$, and $TiAl_{54.5}$ in this paper. They were prepared from high-purity metals by the same procedure as was used by Dimitrov *et al* (1993). The titanium, refined by the iodide (Van Arkel) process, had a very low oxygen level (27 wt ppm) and the main metallic impurities were iron and zirconium ($\approx$100 wt ppm each). The aluminium was a zone-refined material, with a total metallic impurity content

lower than 1 wt ppm.

The alloys were obtained by RF levitation melting under pure helium gas, and casting. To eliminate cracks, the alloys were remelted on a water-cooled copper boat, and directionally solidified. Finally, the ingots were homogenized by annealing in a sealed silica tube evacuated and back-filled with pure helium gas, for 24 hours, at 1400 K; they were wrapped in a tantalum foil 40 μm thick to avoid contamination from silica.

The final compositions were checked by inductively coupled plasma atomic emission spectrometry (ICP-AES) chemical analysis. Some deviations from the nominal compositions were detected, especially for the $TiAl_{51.5}$ compound. Therefore, the actual compositions were evaluated on the basis of the $R_{4.2\,K}/R_{294\,K}$ electrical resistance ratios: the Al concentrations were 50.0, 50.8, 52.7 ± 0.1, and 53.85 ± 0.15, respectively. The alloys were found to be reasonably homogeneous from scanning electron microscope observations with energy-dispersive x-ray analysis. X-ray diffraction and transmission electron microscopy showed that the alloys had an $L1_0$ structure, and each comprised a single γ-phase, except for there being a small amount of α_2-Ti_3Al phase in the stoichiometric $TiAl_{50}$ compound.

Specimens were prepared by cutting slices 800 μm thick from the alloy ingots with a diamond saw, then thinning them to 200–300 μm by mechanical polishing. After subsequent chemical etching, the samples were annealed in a vacuum of 10^{-6} Pa for 10 h at 1223 K and slowly cooled. Pure nickel samples, used as a reference in the irradiation experiments, were prepared by spark machining from material cold-rolled to a thickness of $\approx$30 μm. After chemical etching, they were similarly annealed for 2 h at 1073 K.

Two irradiation experiments were performed with 2.5 MeV electrons at 21 K, in the liquid hydrogen cryostat of the Van de Graaf electron accelerator at the SESI, Ecole Polytechnique, Palaiseau (France). The electron flux density was $\approx 1.4 \times 10^{14}$ electrons cm^{-2} s^{-1}. In the first irradiation (I), a reference pure nickel specimen and three TiAl samples (with 50, 53, and 54.5 at.% Al) were simultaneously irradiated; the fluence was $\approx 1 \times 10^{19}$ electrons cm^{-2} for the Ni and $TiAl_{50}$ samples. Due to a technical problem, the fluence was slightly lower for the $TiAl_{54.5}$ sample and very much lower for the $TiAl_{53}$ sample. In the second experiment (II), four γ-TiAl samples (containing 50, 51.5, 53, and 54.5 at.% Al) were irradiated at a fluence of 8×10^{18} electrons cm^{-2}. The radiation damage was investigated by means of electrical resistivity determinations performed at 21 K using standard four-point DC measurements. The shape factors of the samples, $k = \rho_{4.2\,K}/R_{4.2\,K}$, were deduced from their 4.2 K electrical resistances before irradiation using resistivity values determined for separate specimens of suitable shape ($\approx$1 mm^2 in section), annealed in the same conditions as above. The shape factor of the nickel sample was calculated from the nickel ideal resistivity at 296 K ($\rho_i = 7.04$ $\mu\Omega$ cm), by using the relationship $k = \rho_i/(R_{296\ K} - R_{4.2\ K})$. The uncertainty on the resistivity variations was 1×10^{-9} Ω cm.

For investigating the recovery behaviour, the irradiated samples were isochronally annealed, between 21 and 300 K, in a furnace located inside the cryostat above the liquid hydrogen bath. At higher temperatures, isochronal anneals were carried out in a stainless steel tube immersed in an oil bath between 300 and 435 K (or in a molten salt bath above 435 K), under a reduced pressure of high-purity helium gas, or under a vacuum at the highest temperatures. After irradiation, the samples were pulse annealed with a mean rate of temperature increase of 1.5 K min^{-1}, in steps ranging from 8 min every 12 K to 20 min every 30 K. The recovery of the radiation damage was also investigated by means of electrical resistivity measurements performed at 21 K for the annealings at up to 300 K and at 4.2 K for the annealings at temperatures higher than 300 K. All of the resistivity values measured at 21 K were corrected and reduced to 4.2 K values.

3. Electron irradiation damage

3.1. Experimental results

Electron irradiation produced an increase in resistivity both in the pure nickel and in the γ-TiAl compounds. Figure 1 gives an example of this variation as a function of fluence Φ for the pure nickel and for the $TiAl_{50}$ alloy during irradiation I. The other γ-TiAl compounds irradiated to various fluences displayed a similar behaviour: the curves exhibit an increase of the resistivity with Φ. However, the radiation-induced resistivities $\Delta\rho_i$ were larger by a factor of $\approx$10 in the γ-TiAl alloys than in pure nickel. Furthermore, there is an effect of alloy composition on the excess resistivity in the samples irradiated to the same fluence (irradiation II). The value is largest for the stoichiometric $TiAl_{50}$ alloy, and goes through a minimum for 53 at.% Al (table 1).

Table 1. The residual resistivity of unirradiated materials ρ_0, fluence Φ, and excess resistivity induced by irradiation $\Delta\rho_i$ in pure nickel and in the γ-TiAl compounds, for the two electron irradiations.

	Materials:	Ni	$TiAl_{50}$	$TiAl_{51.5}$	$TiAl_{53}$	$TiAl_{54.5}$
	ρ_0 ($\mu\Omega$ cm):	0.728 ± 0.001	6.67 ± 0.15	17.4 ± 0.4	41.3 ± 0.9	63.4 ± 1.4
Irradiation I	Φ (electrons cm^{-2})	1×10^{19}	1×10^{19}	—	$\approx 3 \times 10^{18}$	$\approx 8.9 \times 10^{18}$
	$\Delta\rho_i$ ($\mu\Omega$ cm)	0.230 ± 0.001	2.140 ± 0.015	—	0.519 ± 0.006	1.642 ± 0.028
Irradiation II	Φ (electrons cm^{-2})	—	8×10^{18}	8×10^{18}	8×10^{18}	8×10^{18}
	$\Delta\rho_i$ ($\mu\Omega$ cm)	—	1.573 ± 0.006	1.532 ± 0.005	1.465 ± 0.008	1.525 ± 0.009

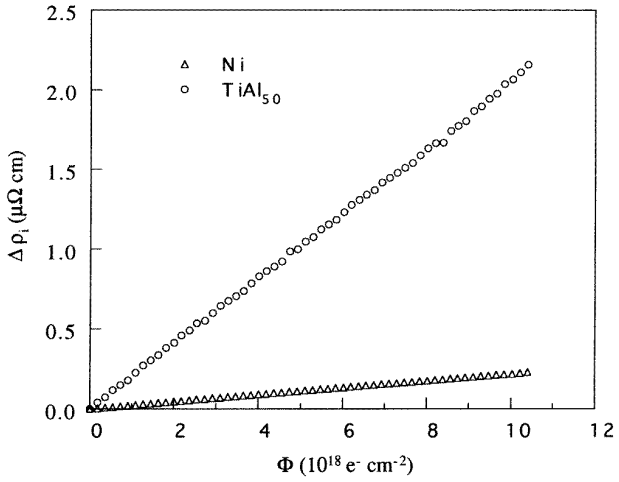

Figure 1. Resistivity variations during 21 K electron irradiation of pure nickel and of the $TiAl_{50}$ alloy (irradiation I).

The resistivity damage rates $d\rho/d\Phi$ were evaluated as functions of the radiation-induced resistivity. The data (figure 2, irradiation II) were fitted to a linear relationship:

$$\dot{\rho} \equiv d\rho/d\Phi = \sigma_d \rho_F [1 - 2\nu_0(\Delta\rho/\rho_F)] \quad (1)$$

where σ_d is the displacement cross section, ρ_F the Frenkel-pair resistivity, and ν_0 the vacancy–interstitial spontaneous recombination volume. Such an equation is of course strictly valid only for pure metals in the case of low defect concentrations. Extrapolation of the curves to zero fluence gives experimental values of the initial resistivity damage rate $(d\rho/d\Phi)_0$ at $\Delta\rho_i = 0$. These were found (table 2) to exhibit a composition dependence similar to that of the final excess resistivities (table 1). The slopes of the linear damage curves appear to become less negative when the aluminium content increases. The saturation resistivity values $\Delta\rho_s$ (corresponding to a damage rate $d\rho/d\Phi$ equal to 0) were unreliable due to the relatively low fluences used in our experiments.

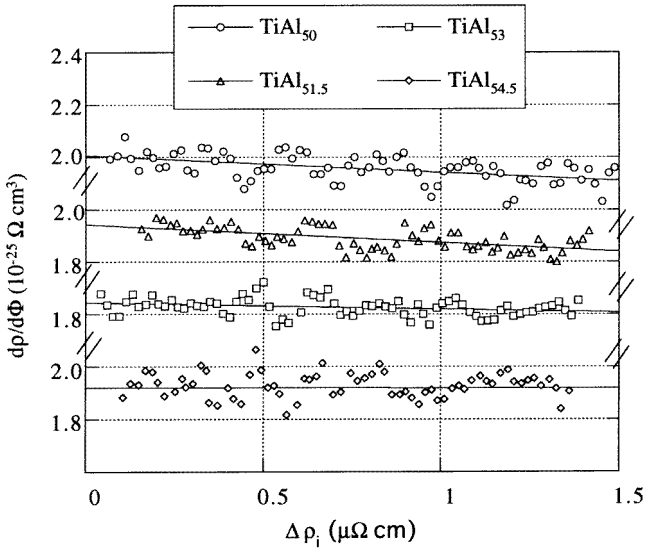

Figure 2. Resistivity damage rates as functions of the irradiation-induced resistivity in the γ-TiAl compounds irradiated to 8×10^{18} electrons cm^{-2}, and least-squares fits of equation (1) to the data.

Table 2. Initial damage rates $(d\rho/d\Phi)_0^{exp}$, relative displacement cross sections, and apparent Frenkel-pair resistivities (neglecting disordering effects) for γ-TiAl compounds.

	Materials:	Ni	$TiAl_{50}$	$TiAl_{51.5}$	$TiAl_{53}$	$TiAl_{54.5}$
Irradiation I	$\dot{\rho}_0^{exp}$ (10^{-25} Ω cm^3)	0.234 ± 0.001	2.06 ± 0.03	—	—	—
	$\sigma_d^{Ni}/\sigma_d^{alloy}$	1	1.144	—	—	—
	ρ_F ($\mu\Omega$ cm/%)	6.7 ± 0.4	68 ± 5	—	—	—
Irradiation II	$\dot{\rho}_0^{exp}$ (10^{-25} Ω cm^3)	—	2.01 ± 0.03	1.94 ± 0.03	1.84 ± 0.03	1.93 ± 0.03
	$\sigma_d^{TiAl_{50}}/\sigma_d^{alloy}$	—	1	1.003	1.007	1.011
	ρ_F ($\mu\Omega$ cm/%)	—	68 ± 5	66 ± 5	63 ± 5	66 ± 5

3.2. Damage processes, and the evaluation of Frenkel-pair resistivities

Point defect creation and disordering of the γ-TiAl compounds, which both lead to a resistivity increase, could be effective during electron irradiation. However, it is difficult to separate directly the contribution to the resistivity arising from the point defects from that due to the disordering, since the results cannot be compared to data on disordered γ- TiAl alloys. Such completely disordered γ-TiAl is impossible to obtain by the usual methods, because the structure remains long-range ordered up to the melting temperature. Therefore, an upper limit for the Frenkel-pair resistivities ρ_F of the γ-TiAl compounds will be first determined by assuming a negligible disordering contribution; then this contribution to the resistivity will be evaluated by two different methods, and subtracted from the experimental data, in order to obtain the point defect contribution.

3.2.1. Evaluation of ρ_F under the assumption of negligible disordering. An evaluation of the Frenkel-pair resistivity ρ_F by the application of equation (1) ($\dot{\rho}_0 = \sigma_d \rho_F$) requires us to know with accuracy the absolute displacement cross section. So instead, we have used a relative method which involves comparing the initial resistivity damage rate for the stoichiometric γ-TiAl to the initial resistivity damage rate for the reference nickel sample, for which ρ_F (6.7 ± 0.4 $\mu\Omega$ cm) is known (Dimitrov and Dimitrov 1985), irradiated in the same experiment (irradiation I):

$$\rho_F^{TiAl_{50}} = [\sigma_d^{Ni}/\sigma_d^{TiAl_{50}}][\dot{\rho}_0^{TiAl_{50}}/\dot{\rho}_0^{Ni}]\rho_F^{Ni}. \tag{2}$$

We used fcc nickel as a reference, because the hexagonal titanium did not seem appropriate for comparison with tetragonal γ-TiAl (which has a ratio c/a very close to 1, and is thus nearly fcc). Fcc aluminium was also not used because of its very low residual resistivity, which could result in significant deviations from Matthiessen's rule during irradiation.

The initial resistivity damage rates for the off-stoichiometric alloys were compared to that for the stoichiometric compound irradiated under the same conditions (irradiation II):

$$\rho_F^{alloy} = [\sigma_d^{TiAl_{50}}/\sigma_d^{alloy}][\dot{\rho}_0^{alloy}/\dot{\rho}_0^{TiAl_{50}}]\rho_F^{TiAl_{50}}. \tag{3}$$

This relative method is used to reduce the uncertainties in the absolute fluence values and in the displacement cross sections. The latter were determined for the γ-TiAl compounds containing x at.% of aluminium by using the expression

$$\sigma_d^{alloy} = (x/100)\sigma_d^{Al} + [(100 - x)/100]\sigma_d^{Ti} \tag{4}$$

The values of $\sigma_d^{Ni}, \sigma_d^{Al}$, and σ_d^{Ti} were calculated from Oen's tabulation (Oen 1973) by adopting the effective average atomic threshold displacement energies of the pure elements evaluated for a fcc lattice according to Lucasson (1975): 33 eV for nickel, 27 eV for aluminium, and 28.5 eV for titanium.

Thus, without taking into account a disordering contribution, an upper limit for the Frenkel-pair resistivities can be evaluated from equation (2) for the stoichiometric alloy with reference to the initial damage rates for pure nickel alloy, and from equation (3) for the off-stoichiometric alloys with reference to the stoichiometric one (table 2).

3.2.2. Estimation of ρ_F with an evaluation of the disordering contribution to the radiation damage. In long-range-ordered γ-TiAl, disordering results from the formation of antisite defects, produced mainly by atomic replacement collisions: at the temperature of the irradiation (21 K), spontaneous interstitial–vacancy recombinations should be limited.

The experimental initial damage rate $(\mathrm{d}\rho/\mathrm{d}\Phi)_0^{\mathrm{exp}}$ was considered as a sum of two contributions, one due to point defect production $(\mathrm{d}\rho/\mathrm{d}\Phi)_0^{\mathrm{def}}$ and the other assigned to disordering, i.e. antisite defects created by atomic replacement collisions $(\mathrm{d}\rho/\mathrm{d}\Phi)_0^{\mathrm{dis}}$:

$$(\mathrm{d}\rho/\mathrm{d}\Phi)_0^{\mathrm{exp}} = (\mathrm{d}\rho/\mathrm{d}\Phi)_0^{\mathrm{def}} + (\mathrm{d}\rho/\mathrm{d}\Phi)_0^{\mathrm{dis}}. \tag{5}$$

The disordering contribution was evaluated by two different methods:

(i) a theoretical evaluation, which requires the introduction of a number of poorly known parameters; and

(ii) a phenomenological evaluation, which relies on the assumption of a specific composition dependence of the two contributions (point defects and disordering) to the resistivity variations induced by irradiation.

(a) Theoretical evaluation of disordering induced by irradiation

The initial damage rate $(\mathrm{d}\rho/\mathrm{d}\Phi)_0^{\mathrm{dis}}$ due to atomic replacement collisions can be written as (Dimitrov *et al* 1992a):

$$(\mathrm{d}\rho/\mathrm{d}\Phi)_0^{\mathrm{dis}} = (\mathrm{d}\rho/\mathrm{d}S)_0(\mathrm{d}S/\mathrm{d}C_{\mathrm{R}})_0(\mathrm{d}C_{\mathrm{R}}/\mathrm{d}C_{\mathrm{D}})_0(\mathrm{d}C_{\mathrm{D}}/\mathrm{d}\Phi)_0 \tag{6}$$

where S is the long-range-order (LRO) parameter; indices R and D refer respectively to replaced and displaced atoms; $\mathrm{d}\rho/\mathrm{d}S$ is the contribution to the resistivity of a change in the LRO parameter S; $\mathrm{d}S/\mathrm{d}C_{\mathrm{R}}$ corresponds to the variation of the LRO parameter S induced by a change in the concentration C_{R} of the atomic replacements; $\mathrm{d}C_{\mathrm{R}}/\mathrm{d}C_{\mathrm{D}}$ is the average number of replacements per displacement; and $\mathrm{d}C_{\mathrm{D}}/\mathrm{d}\Phi$ is the production rate of Frenkel defects. These parameters were determined as follows.

(i) $(\mathrm{d}\rho/\mathrm{d}S)_0$. For the order-dependent residual electrical resistivity in a long-range ordered alloy, a generalized version (Dimitrov *et al* 1992c) of the relationship given by Rossiter (1980) was used:

$$\rho(S) = (\rho_{\mathrm{dis}} - \rho_{\mathrm{ord}})(1 - (S/S_{\mathrm{max}})^2)/(1 - A(S/S_{\mathrm{max}})^2) \tag{7}$$

where S is the Bragg–Williams LRO parameter, ρ_{dis} the resistivity of the disordered alloy, ρ_{ord} the residual resistivity corresponding to the maximum degree of order, S_{max} the maximum value of the LRO parameter, and A a parameter depending on the electronic structure of the material. Differentiating equation (7) gives for $S_0 = S_{\mathrm{max}}$, at the beginning of the irradiation,

$$(\mathrm{d}\rho/\mathrm{d}S)_0 = -2(\rho_{\mathrm{dis}} - \rho_{\mathrm{ord}})/(1 - A)S_{\mathrm{max}}. \tag{8}$$

This expression was evaluated by the following method.

(1) First, the variation with temperature of the equilibrium LRO parameter S of the γ-TiAl alloys was evaluated in the Bragg–Williams approximation (Krivoglaz and Smirnov 1964, Badura and Schaefer 1993). This leads to the following expression:

$$\ln[(1 + 2\delta + S)(1 - 2\delta + S)/(1 + 2\delta - S)(1 - 2\delta - S)] = 4S(T_{\mathrm{c}}/T)[1/(1 - 4\delta^2)] \tag{9}$$

with T_{c} the critical temperature of the order–disorder transition, and $\delta = C_{\mathrm{Al}} - 0.5$ the deviation from stoichiometry. The critical temperature T_{c} of the order–disorder transition was evaluated from the experimentally determined LRO parameter S of splat-cooled stoichiometric γ-TiAl (Vujic *et al* 1988), assuming that it was representative of the order state at the melting temperature.

(2) Secondly, the temperature dependence of the residual resistivity of unirradiated alloys, in the temperature range where they are representative of the equilibrium LRO, were deduced from the results of Dimitrov *et al* (1996).

Table 3. Estimated values of T_c and values of ρ_{ord}, ρ_{dis}, and A determined by fitting equation (10) to the temperature dependence of the residual electrical resistivity of the unirradiated alloys.

Alloys	T_c (K)	ρ_{ord} ($\mu\Omega$ cm)	ρ_{dis} ($\mu\Omega$ cm)	A
$TiAl_{50}$	1849	0.03	21.50	0.829
$TiAl_{51.5}$	1847	15.68	31.53	0.851
$TiAl_{53}$	1842.5	41.10	43.45	0.897
$TiAl_{54.5}$	1834	63.23	66.64	0.914

From these two sets of data, it was possible to derive a $\rho = f(S)$ relationship for each alloy, and obtain values of ρ_{ord}, ρ_{dis}, and A (table 3) by fitting the expression

$$\rho = \rho(S) + \rho_{ord} \tag{10}$$

with $\rho(S)$ given by equation (7).

$(d\rho/dS)_0$ was calculated for each alloy by introducing these values in equation (8). It should be noted that this method is not fully satisfactory, because ρ_{dis} is found to be low in the $TiAl_{50}$ alloy, and to vary strongly with the composition. This is not expected in the restricted composition range of the present set of alloys.

(ii) $(dS/dC_R)_0$. A calculation similar to the one performed by Becker *et al* (1968) for $L1_2$ crystal was performed for the $L1_0$ stoichiometric γ-TiAl, by considering the relationship between S and the number of replacement collisions in $\langle 110 \rangle$ rows. It gives

$$(dS/dC_R)_0 = -(4/3)S_{max}.$$

(iii) $(dC_R/dC_D)_0$. The average number of replacements per displacement at the beginning of the irradiation was taken to be equal to 3 ± 1, by analogy with Ni_3Al, another fcc-based intermetallic compound (Dimitrov *et al* 1992a).

Table 4. The Frenkel-pair resistivities ρ_F of the γ-TiAl compounds obtained by estimating the disordering contribution by two different methods (see the text), residual electrical resistivity variations assigned to LRO changes during thermal treatments $\Delta\rho_{th}$ (from data given by Dimitrov *et al* 1996), and initial damage rates $\dot{\rho}_0$ ('exp' = experimental, 'dis' = estimated disordering contribution, 'def' = resulting defect contribution).

Evaluation of disordering contribution	Irradiation:	I	II			
	Alloys:	$TiAl_{50}$	$TiAl_{50}$	$TiAl_{51.5}$	$TiAl_{53}$	$TiAl_{54.5}$
Theoretical	ρ_F ($\mu\Omega$ cm/%)	58 ± 7	56 ± 7	56 ± 7	59 ± 7	61 ± 7
Phenomenological	$\Delta\rho_{th}$ ($\mu\Omega$ cm)		0.66	0.65	0.14	0.21
	$\dot{\rho}_0^{exp}$ (10^{-25} Ω cm^3)		2.01 ± 0.03	1.94 ± 0.03	1.84 ± 0.03	1.93 ± 0.03
	$\dot{\rho}_0^{dis}$ (10^{-25} Ω cm^3)		0.17	0.17	0.04	0.05
	$\dot{\rho}_0^{def}$ (10^{-25} Ω cm^3)		1.80 ± 0.07	1.82 ± 0.07	1.83 ± 0.07	1.85 ± 0.07
	ρ_F ($\mu\Omega$ cm/%)		61 ± 6	62 ± 6	63 ± 6	63 ± 6

(iv) $(dC_D/d\Phi)_0$. This term represents the displacement cross section for γ-TiAl, it was evaluated with reference to pure nickel by using the relationship:

$$(dC_D/d\Phi)_0 \equiv \sigma_d^{TiAl} = (\sigma_d^{TiAl}/\sigma_d^{Ni})_{Oen}(\dot{\rho}_0^{Ni}/\rho_F^{Ni}). \tag{11}$$

From the numerical values (table 2), it turns out that for the stoichiometric compound

$$\sigma_d^{TiAl} = 30 \pm 2 \text{ b}.$$

The contribution of disordering to the total resistivity damage rate $(d\rho/d\Phi)_0^{dis}$ was determined by introducing in equation (6) the different factors evaluated above.

Finally, the initial resistivity damage rates due to defect production $(d\rho/d\Phi)_0^{def}$ were calculated by subtracting $(d\rho/d\Phi)_0^{dis}$ from the experimentally determined initial damage rates. Then, the Frenkel-pair resistivities of the γ-TiAl intermetallic alloys were calculated using equation (2). The results obtained by this theoretical method are reported for each composition in table 4.

(b) Phenomenological evaluation of the disordering induced by irradiation

The contributions of point defects and disordering to the resistivity increase occurring during irradiation were evaluated under the following assumptions.

(i) In the limited concentration range investigated, it was considered that the contribution of point defects to the initial resistivity damage rate displayed a weak monotonic composition dependence, as observed for Ni_3Al intermetallic compounds (Dimitrov *et al* 1992a). This dependence was assumed to be linear:

$$(d\rho/d\Phi)_0^{def} = k_0 + k_1 C_{Al} \tag{12}$$

where C_{Al} is the aluminium concentration of the compound.

(ii) The experimental initial damage rates ($\dot{\rho}_0^{exp}$) in irradiation II (table 2) display a composition dependence, with a minimum at 53 at.% Al. This trend is similar to that of the variations of the resistivity with temperature assigned to thermal disordering in unirradiated γ-TiAl compounds (Dimitrov *et al* 1996). Consequently, the disordering contribution to the resistivity damage rate was assumed to be proportional to the amplitude of the resistivity variations connected with thermal LRO changes:

$$(d\rho/d\Phi)_0^{dis} = k_2 \, \Delta\rho_{th} \tag{13}$$

where $\Delta\rho_{th}$ is the change in the equilibrium order resistivity of each alloy, determined in the temperature interval common to the four TiAl compounds (900–930 K).

Therefore, k_0, k_1, and k_2 were determined by fitting the following equation to the experimental $\dot{\rho}_0^{exp}$-values (irradiation II, table 2) and to the values of $\Delta\rho_{th}$ (table 4):

$$\dot{\rho}_0^{exp} = k_0 + k_1 C_{Al} + k_2 \, \Delta\rho_{th}(C_{Al}). \tag{14}$$

This method allows us to determine separately $(d\rho/d\Phi)_0^{def}$ and $(d\rho/d\Phi)_0^{dis}$; the results are reported in table 4.

The two independent evaluations of the disordering contribution to the resistivity damage rate lead to comparable results: $(d\rho/d\Phi)_0^{dis}$ represents 8 to 15% of the initial resistivity damage rate for the stoichiometric alloy, and even less for the high-Al alloys. Thus, this contribution is not negligible, but the dominant effect of electron irradiation is the production of Frenkel defects. The Frenkel-pair resistivities (ρ_F) resulting from the two evaluations are similar, around 60 $\mu\Omega$ cm/%. There might be a slight tendency for ρ_F to increase with the aluminium content. These values are much larger than the Frenkel-pair resistivities of the constituent metals: $\rho_F^{Al} = 4.2$ $\mu\Omega$ cm/% (Ehrhart *et al* 1974), and $\rho_F^{Ti} = 14$–18 $\mu\Omega$ cm/% (Shirley and Chaplin 1972); they are smaller than the values determined for the stoichiometric Ni_3Al intermetallic compound: 102 $\mu\Omega$ cm/% (Dimitrov *et al* 1992a).

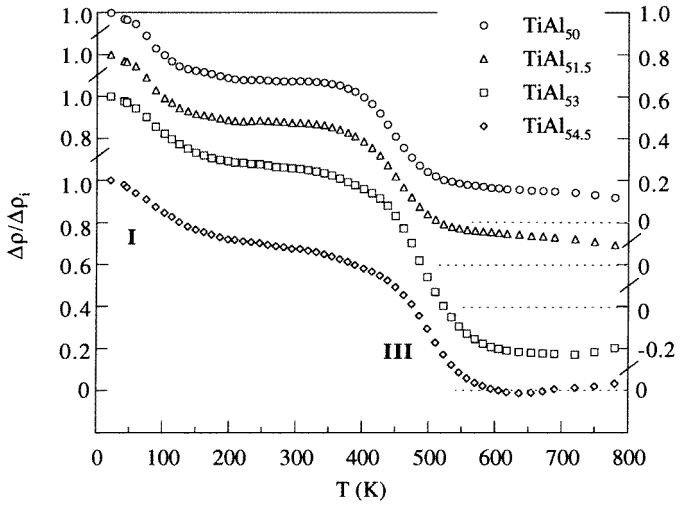

Figure 3. Isochronal resistivity recovery curves of the γ-TiAl compounds irradiated to 8×10^{18} electrons cm^{-2}.

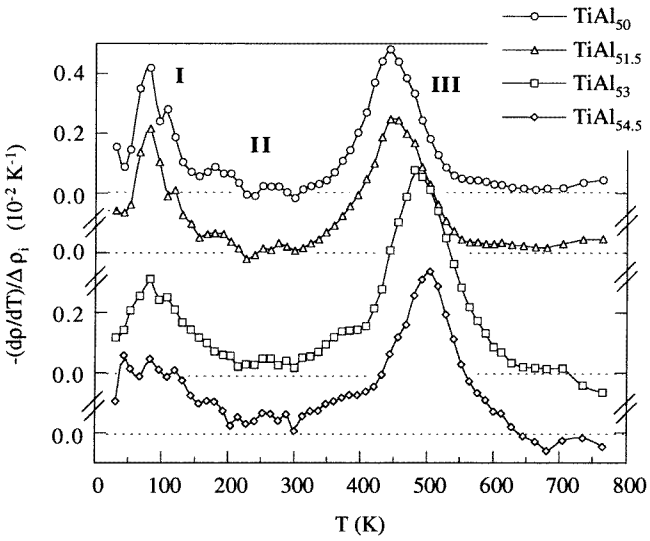

Figure 4. Derivative curves of the isochronal resistivity recovery for the γ-TiAl compounds irradiated to 8×10^{18} electrons cm^{-2}.

4. Recovery after electron irradiation

For the electron-irradiated nickel sample, the isochronal resistivity recovery curve was found to be very similar to those described in the literature (see, for instance, Bartels *et al* 1986). The main features of the recovery are the following.

(i) Stage I (21–70 K), the main recovery stage, is associated with close-pair recombination, and with the correlated and uncorrelated annihilation of mobile interstitials

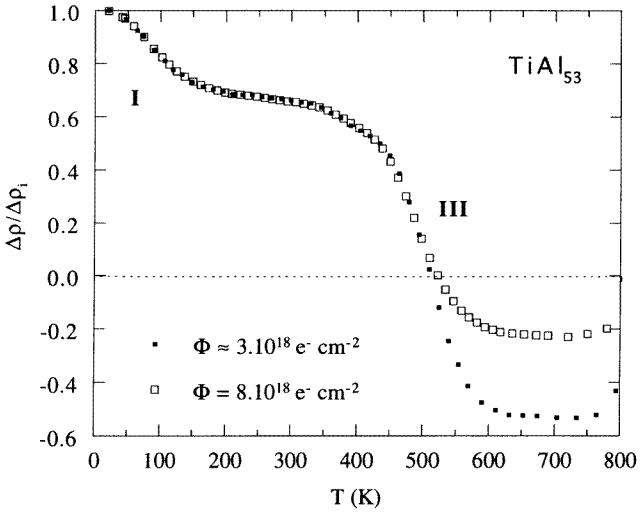

Figure 5. Isochronal resistivity recovery curves of the $TiAl_{53}$ alloy irradiated to $\approx 3 \times 10^{18}$ electrons cm^{-2} and 8×10^{18} electrons cm^{-2}.

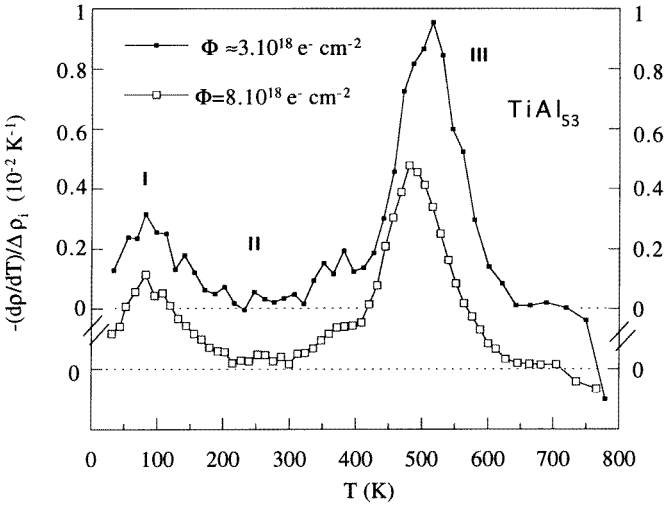

Figure 6. Derivative curves of the isochronal resistivity recovery for the $TiAl_{53}$ alloy irradiated to $\approx 3 \times 10^{18}$ electrons cm^{-2} and 8×10^{18} electrons cm^{-2}.

with vacancies.

(ii) Stage II (70–300 K) displays a fine structure with several substages. It is attributed to the migration, dissociation, or structure rearrangement of small interstitial clusters formed at the end of stage I.

(iii) Stage III appears as a small peak centred at ≈340 K. Positron lifetime measurements (Nguy 1988) showed that it is due to the migration of vacancies. Recovery of the low-temperature-irradiated pure nickel sample is complete at 490 K.

The relative resistivity recovery curves of the four γ-TiAl alloys irradiated to 8×10^{18}

Table 5. Temperatures of the maximum recovery rate T_M, and relative amplitudes of the recovery stages $\Delta\rho/\Delta\rho_i$ of γ-TiAl compounds irradiated to the fluence Φ.

		Stages					
		I (21–150 K)		II (150–300 K)	III (300–660 K)		Total (up to 660 K)
Alloys	Φ (10^{18} electrons cm^{-2})	T_M (K)	$\Delta\rho/\Delta\rho_i$ (%)	$\Delta\rho/\Delta\rho_i$ (%)	T_M (K)	$\Delta\rho/\Delta\rho_i$ (%)	$\Delta\rho/\Delta\rho_i$ (%)
$TiAl_{50}$	10	78	26.6	5.6	443	51.7	83.9
	8	81	27.7	5.1	444	52	84.8
$TiAl_{51.5}$	8	81	28.3	4.2	451	53.9	86.4
$TiAl_{53}$	8	81	26.7	7.5	487	87.8	122
	≈ 3	84	26.9	7	516	118.5	152.4
$TiAl_{54.5}$	8	42–82	23.5	9.1	501	67.4	100

electrons cm^{-2} are shown in figure 3, and those of the $TiAl_{53}$ alloy irradiated to 8×10^{18} and $\approx 3 \times 10^{18}$ electrons cm^{-2} as shown in figure 5. Two major stages of resistivity recovery are observed (denoted as I and III in the figures), and their amplitudes are composition dependent: the ratio of stage III to stage I increases with the aluminium content (table 5). The derivative curves (figures 4 and 6) clearly show the structure of the recovery stages.

For the $TiAl_{50}$ alloy, the first one is found to occur at around 80 K, and involves some substructure. It is followed by a region of weak, progressive recovery (stage II) in which two peaks at 184 K and 268 K can be distinguished. Stage III displays a peak of maximum recovery rate at 444 K. At the end of this stage, a significant excess resistivity is still present, and it disappears only above 800 K.

4.1. The composition dependence of the recovery stages

The effect of aluminium concentration will be discussed with reference to irradiation II. Stage I will be here defined as the recovery extending up to ≈150 K, on the basis of the derivative curve of the $TiAl_{50}$ alloy. This first main recovery stage (23 to 28% of the radiation-induced resistivity according to composition; see table 5) is characterized by a peak at ≈81 K in all alloys, with a shoulder on the high-temperature side for the compositions 50, 51.5, and 53 at.% aluminium. For the $TiAl_{54.5}$ alloy, stage I is more complicated, with the appearance of a pronounced substructure. The temperature of the maximum recovery rate in stage I appears to be independent of the composition, although the shape of the peak varies.

Stage II (150–300 K) represents 4–9% of the initial excess resistivity. The two small substages, identified in $TiAl_{50}$, can also be recognized in $TiAl_{51.5}$ and $TiAl_{54.5}$; only the second one can be seen in the $TiAl_{53}$ alloy. The relative amplitude of this stage tends to increase with aluminium content.

Stage III (300–660 K) is the second main recovery stage (52–118% of the radiation-induced resistivity). Its temperature is composition dependent (table 5), the corresponding peak being shifted to higher temperatures by 60 K when the aluminium content increases from 50 to 54.5 at.% of Al. At the beginning of this temperature range, a progressive recovery takes place just above 300 K; this is more conspicuous for the alloys with a higher aluminium content, probably because of the shift of stage III to higher temperatures. The amplitude of stage III is composition dependent, with a maximum value for the $TiAl_{53}$ alloy.

Beyond stage III, the $TiAl_{50}$ and $TiAl_{51.5}$ alloys show very similar behaviour and, after the last anneal at 780 K, there remain 11.8% and 9.3% respectively of the excess resistivity induced by irradiation. By contrast, the $TiAl_{53}$ alloy over-recovers during stage III, and it displays resistivity values lower than in the unirradiated state. The $TiAl_{54.5}$ alloy recovers its pre-irradiation resistivity value at around 650 K.

4.2. The fluence dependence of the recovery

The effect of the initial defect concentration on the recovery was mainly investigated for the $TiAl_{53}$ alloy. The effect of a decrease of the defect concentration on the temperature of stage I appears marginal, but there might be a tendency for this stage to undergo a slight shift to higher temperatures; the relative amplitude of this stage is independent of the fluence (table 5). By contrast, the effect on the temperature of stage III is strong: a decrease of defect concentration (lower fluence) leads to a shift by 36 K to higher temperatures of stage III, and its relative magnitude is enhanced (figures 5 and 6). However, the maximum decrease of the absolute resistivity below its initial value, around 650 K, is the same for the two fluences.

4.3. The interpretation of the recovery stages

The nature of the defects produced by irradiation in γ-TiAl has not yet been directly investigated. Some likely structures can be predicted, on the basis of the crystal structure of this compound. γ-TiAl has a face-centred tetragonal $L1_0$ structure, which is a superstructure of the fcc lattice with alternating {001} planes containing only Ti or Al atoms. Two types of vacancy should exist in TiAl, according to their position on the Al or Ti sublattices. For self-interstitial defects, a likely configuration is the ⟨100⟩ dumb-bell split interstitial, similarly to the one existing in fcc metals. Three types of dumb-bell can then be produced by irradiation: Ti–Ti (on Ti sites), Ti–Al mixed dumb-bells (distributed on both Ti and Al sites), and Al–Al (on Al sites).

The first broad peak observed in the derivative recovery curves exhibits a maximum recovery rate at ≈81 K; its position is independent of the composition, and possibly slightly dependent on the fluence. By analogy with the recovery of electron-irradiated nickel or Ni_3Al intermetallic compounds (Dimitrov *et al* 1992b), it seems reasonable to assign this stage (stage I) to the recombination of close pairs, and to the correlated and uncorrelated annihilation of mobile self-interstitials with vacancies. A fraction of the mobile interstitials may be trapped at impurity atoms or may form interstitial clusters. However, Hishinuma *et al* (1993) considered that the migration of ⟨100⟩ dumb-bell split interstitials in TiAl (implicitly assumed to be pure Ti–Ti or Al–Al) should be preferentially restricted to the four jump directions in the {001} plane, so as to avoid disturbing the ordered structure. This two-dimensional migration was thought to result in the suppression of the nucleation and growth of interstitial clusters.

Stage II, in the range 150–300 K, includes several substages, which can be clearly seen as distinct peaks of the derivative curves. They could correspond to the annihilation of interstitial defects of lower mobility, or to the dissociation of impurity–interstitial complexes or interstitial clusters.

The second main recovery stage (stage III) has a temperature and an amplitude that are dependent on the fluence and on the composition. It is shifted to lower temperatures with increasing fluence. This indicates a defect reaction with a kinetic order larger than one, and is consistent with the free migration of a point defect. This stage can be reasonably

assigned to the migration of vacancies. Its temperature (444 K for the $TiAl_{50}$ alloy) is much higher than the temperature assigned to vacancy migration by Shirai and Yamaguchi (1992) on the basis of positron lifetime measurements, but it agrees with the interpretation of a decrease of the positron lifetime at around 450 K, in terms of vacancy migration, proposed by Würschum *et al* (1996).

Stage III is shifted to higher temperatures with increasing Al content. In the framework of the above assignment, such a shift shows that the vacancy mobility (i.e. the vacancy jump frequency ν_V) decreases when the aluminium concentration increases. This result can be compared with the recent characterization of the atomic mobility in the same alloys (Dimitrov *et al* 1996); it was found that atomic jump frequency increased with the aluminium content. Since the atomic jump frequency (ν_{at}) and the vacancy jump frequency (ν_V) are related to the equilibrium vacancy concentration $C_V(T)$ at temperature T by the expression

$$\nu_{at} = \nu_V C_V(T) \tag{15}$$

we can deduce a composition dependence of the vacancy concentration. From (15), it turns out that the vacancy concentration at a given temperature increases with aluminium content; therefore, the vacancy formation enthalpy (H_V^F) decreases, according to the relation between C_V and H_V^F:

$$C_V(T) \propto \exp(-H_V^F/kT). \tag{16}$$

This experimental conclusion supports the theoretical predictions of Badura and Schaefer (1993) and Fu and Yoo (1993) concerning the composition dependence of the vacancy formation enthalpy in γ-TiAl intermetallic compounds.

The effective enthalpy of vacancy migration (H_V^M) in stoichiometric γ-TiAl can be estimated from the temperature which characterizes stage III (444 K), by comparison with the data (temperature and vacancy migration enthalpy) obtained for stage III for stoichiometric Ni_3Al (Dimitrov *et al* 1992b). We assumed that the vacancy elimination involves a similar migration entropy, and requires similar numbers of jumps in the two intermetallic compounds. This estimation leads to $H_V^M = 1.55 \pm 0.16$ eV for stoichiometric γ-TiAl. This value is in good agreement with the one (1.59 eV) proposed by Würschum *et al* (1996) from the difference between the Ti self-diffusion enthalpy and the vacancy formation enthalpy values in TiAl.

5. Conclusion

The damage produced by 2.5 MeV electron irradiation at 21 K, in stoichiometric and in Al-rich off-stoichiometric γ-TiAl compounds, was investigated by means of electrical resistivity measurements. The contribution of the disordering to the radiation-induced resistivity appears to be significant but not dominant, as compared to the defect resistivity. The Frenkel-pair resistivity values for the TiAl alloys ($\approx$60 $\mu\Omega$ cm/%) are larger than those of pure metals, but smaller than the ones evaluated for Ni_3Al intermetallic compounds.

The recovery of electron irradiation damage in the γ-TiAl intermetallics was also investigated by electrical resistivity measurements. Two major stages of recovery were observed. The first one (at around 81 K) can be assigned to close-pair recombination, and to the migration and annihilation of self-interstitials; the second one (centred at 444 K in the stoichiometric compound) can be attributed to the migration and elimination of vacancies with an estimated activation enthalpy of 1.55 ± 0.16 eV. The temperature of this latter stage is composition dependent; with increasing aluminium concentration, it is shifted to higher temperatures, indicating a reduction in vacancy mobility.

Acknowledgments

The authors would like to thank J L Bonnentien (CECM) for the preparation of the materials, J L Pastol (CECM) for the scanning electron microscope observations, and Dr M Fedoroff and J C Rouchaud (CECM) for the ICP/AES analyses. They are grateful to Dr F Rullier-Albenque (SESI) for providing them with the opportunity to use the electron irradiation facility, and to J Ardonceau (SESI) for help during the irradiations.

References

Badura K A and Schaefer H E 1993 *Z. Metallk.* **84** 405–9
Bartels A, Dworschak F and Weigert M 1986 *J. Nucl. Mater.* **137** 130–8
Becker D, Dworschak F, Lehmann C X, Rie K T, Schuster H, Wollenberger H and Wurm J 1968 *Phys. Status Solidi* **30** 219–29
Brossmann U, Würschum R, Badura K A and Schaefer H E 1994 *Phys. Rev.* B **49** 6457–61
Dimitrov C and Dimitrov O 1985 *Radiat. Eff.* **84** 117–29
Dimitrov C, Martin N, Fekkar H and Dimitrov O 1996 *Scr. Metall.* **34** 1405–9
Dimitrov C, Pastol J-L, Bigot J and Dimitrov O 1993 *J. Physique IV, Coll.* (supplement to *J. Physique* III) **3** C7 481–4
Dimitrov C, Sitaud B, Zhang X, Dimitrov O, Dedek U and Dworschak F 1992a *J. Phys.: Condens. Matter* **4** 10 199–210
——1992b *J. Phys.: Condens. Matter* **4** 10 211–26
Dimitrov C, Tarfa T and Dimitrov O 1992c *Ordering and Disordering in Alloys* ed A R Yavari (London: Elsevier Applied Science) p 130
Ehrhart P, Haubold H G and Schilling W 1974 *Adv. Solid State Phys.* **14** 87
Fu C L and Yoo M H 1993 *Intermetallics* **1** 59–63
Hirano K and Iijima Y 1984 *Diffusion in Solids: Recent Developments; Conf. Proc.* ed M A Dayananda and G E Murch (Detroit, MI: Metallurgical Society of the AIME) p 141
Hishinuma A, Nakata K, Fukai K, Ameyama K and Tokizane M 1993 *J. Nucl. Mater.* **199** 39–46
Krivoglaz M A and Smirnov A A 1964 *The Theory of Order–Disorder in Alloys* (London: MacDonald) p 141
Kroll S, Mehrer H, Stolwijk N, Herzig C, Rosenkranz R and Frommeyer G 1992 *Z. Metallk.* **83** 591–5
Lucasson P 1975 *Fundamental Aspects of Radiation Damage in Metals* vol 1, ed M T Robinson and F W Young Jr (Oak Ridge, TN: Oak Ridge National Laboratory) p 42
Mori S, Miura H, Yamagazy S, Suzuki T, Shimizu A, Seki Y, Kunugi T, Nishio S, Fujisawa N, Hishinuma A and Kikuchi M 1992 *Fusion Technol.* **21** 1744–8
Nguy T 1988 *Thesis* University Paris XI
Oen O S 1973 *Oak Ridge National Laboratory Report* ORNL-4897
Rossiter P L 1980 *J. Phys. F: Met. Phys.* **10** 1459–65
Shirai Y, Kohda H, Murakami T, Yamaguchi M and Kodaka H 1996 *Intermetallics* **4** 139–42
Shirai Y and Yamaguchi M 1992 *Mater. Sci. Eng.* A **152** 173–81
Shirley C G and Chaplin R L 1972 *Phys. Rev.* B **5** 2027–9
Sprengel W, Oikawa N and Nakajima H 1996 *Intermetallics* **4** 185–9
Vujic D, Li Zhixian and Whang Sung H 1988 *Metall. Trans.* A **19** 2445–55
Würschum R, Badura-Gergen K, Kümmerle E A, Grupp C and Schaefer H-E 1996 *Phys. Rev.* B **54** 849–56